Steel and Composite Structures, *Vol. 30, No. 2 (2019) 185-199*
DOI: https://doi.org/10.12989/scs.2019.30.2.185

Stability study on tenon-connected SHS and CFST columns in modular construction

Yisu Chen [a], Chao Hou [*] and Jiahao Peng [b]

School of Civil Engineering, The University of Sydney, Sydney, NSW 2006, Australia

(*Received September 11, 2018, Revised January 22, 2019, Accepted January 23, 2019*)

Abstract. Modular construction is an emerging technology to accommodate the increasing restrictions in terms of construction period, energy efficiency and environmental impacts, since each structural module is prefabricated offsite beforehand and assembled onsite using industrialized techniques. However, some innate structural drawbacks of this innovative method are also distinct, such as connection tying inaccessibility, column instability and system robustness. This study aims to explore the theoretical and numerical stability analysis of a tenon-connected square hollow section (SHS) steel column to address the tying and stability issue in modular construction. Due to the excellent performance of composite structures in fire resistance and buckling prevention, concrete-filled steel tube (CFST) columns are also taken into account in the analysis to evaluate the feasibility of adopting composite sections in modular buildings. Characteristic equations with three variables, i.e., the length ratio, the bending stiffness ratio and the rotational stiffness ratio, are generated from the fourth-order governing differential equations. The rotational stiffness ratio is recognized as the most significant factor, with interval analysis conducted for its mechanical significance and domain. Numerical analysis using ABAQUS is conducted for validation of characteristic equations. Recommendations and instructions in predicting the buckling performance of both SHS and CFST columns are then proposed.

Keywords: modular construction; tenon-connected column; square hollow section (SHS); concrete-filled steel tube (CFST); buckling analysis

1. Introduction

Modular construction is an emerging construction technology in building industry worldwide (Annan 2008, Gunawardena *et al*. 2016b, Lacey *et al*. 2018). This new construction technology has gained increasing attention in engineering practice due to its innovative construction procedures and relevant inherent advantages, such as time and cost efficiency (Lawson *et al*. 2012, Taghaddos *et al*. 2014), superior product qualities (Shahtaheri *et al*. 2017), higher safety (Court *et al*. 2009), excellent thermal and acoustic insulation performances (Matoski and Ribeiro 2016), and less environmental impacts (Jaillon *et al*. 2009, Quale *et al*. 2012), etc. Attributed to these structural benefits, the application of modular construction in practice is growing rapidly, with its typical applications in multilayer buildings presented in Figs. 1(a)-(b).

Lawson *et al*. (2014) reported several case studies on successful application of modular construction in forms of residential buildings, student accommodations, hotels and hospitals. The highly repetitive layout of these buildings allowed the advantages of modular construction to be maximized. To consider the life cycle performance of modular buildings, a thorough study on the sustainability benefits arisen from modular construction has been conducted by Kamali and Hewage (2016), where it is suggested that modular buildings are expected to be more environmentally friendly than their conventional counterparts. Lacey *et al*. (2018) and Pang *et al*. (2016) comprehensively reviewed the structural response of modular buildings and concluded that the structural performance of a modular system was heavily dependent on the connections, especially the inter-connections that linked the adjacent modules together.

Besides the well-recognized structural benefits stated above, modular buildings possess their own disadvantages compared with conventional steel or reinforced concrete structures, which can be grouped into three main aspects: manufactory-constructional drawbacks, architectural drawbacks and structural drawbacks. Manufactory-constructional issues mainly refers to the high requirements on accuracy in manufacture and installation as well as the high demands for crane capacity for higher levels of modularization (Lawson *et al*. 2014, 2016), which could be resolved with more precise and advanced manufactural and lifting equipment. Architectural issues such as the limited internal spaces and planning variation indicate that particular attention is needed in the design of modular construction due to this inherent drawback (Smith 2011). It should be noted that, structural issues are among the most distinct shortcomings in modular construction and need to be addressed properly to ensure the safety and quality of the structure. Typical structural issues in modular construction include instability, robustness and internal tying problems

∗Corresponding author, Ph.D.,
E-mail: chao.hou@sydney.edu.au; houc05@foxmail.com
[a] Master Student, E-mail: yche8685@uni.sydney.edu.au
[b] Ph.D. Student, E-mail: jpen8174@uni.sydney.edu.au

http://www.techno-press.org/?journal=scs&subpage=6
ISSN: 1229-9367 (Print), 1598-6233 (Online)

(a) Installation of a module building at London

(b) A modular residnce construction at Tianjin

Fig. 1 Typical applications of modular construction (Lawson and Ogden 2008. Chen *et al*. 2017)

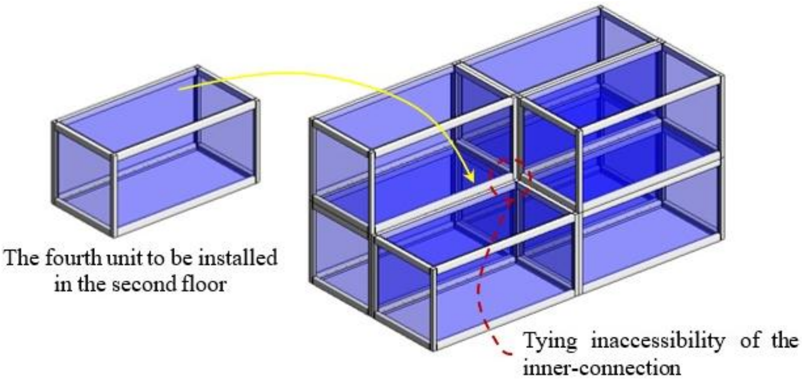

Fig. 2 Schematic view of a typical inner connection in modular construction

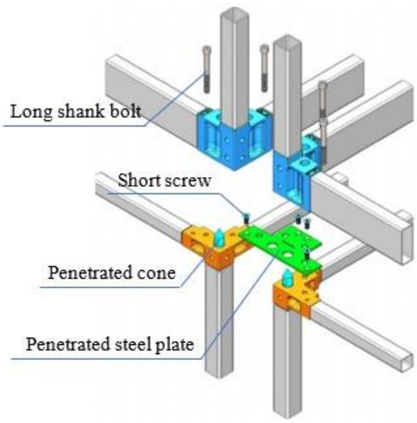

(a) Schematic view

(b) Practical photo

Fig. 3 An existing configuration of inner connections for modular construction (Vector Praxis 2011)

(Lawson *et al*. 2014, Choi and Kim 2014, Gunawardena *et al*. 2016a, Chen *et al*. 2017a, b, Chua *et al*. 2018).

In steel modular system, different modules are connected vertically and horizontally to form tying action either through bolting or welding at the eight corners of each cuboid frame. However, the internal tying could be problematic owing to the inaccessibility of connecting measures like bolting or welding at the inner connection when assembling the last module, as illustrated in Fig. 2. To overcome the internal tying issue, Canadian design company Vector Praxis (2011) has developed a new connecting method using a set of connection components to achieve horizontal and vertical inter-unit tying actions, as presented in Fig. 3. As shown in Fig. 3, penetrated cones, penetrated steel plates, long shank bolts and short screws are adopted in the connection. However, for modular building with higher stories, this type of connection can be relatively weak due to the discreteness of these components. To further guarantee the integrity of the connection in modular construction, Deng *et al*. (2017) proposed a novel connection method. As shown in Fig. 4, an independent connector consisting of a gusset plate and socket tenons is

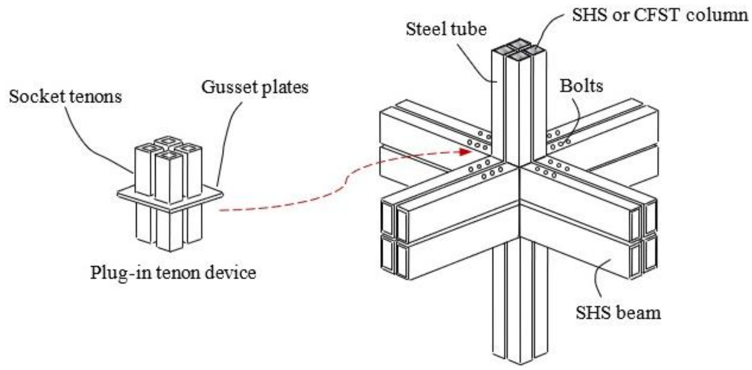

Fig. 4 Schematic view of the inner connection using tenon and gusset plate

prefabricated in factory. The connector is then used together with a set of penetrations perforated offsite for bolt connections between columns and beams of adjacent modules after their preliminary installation onsite.

Another structural shortcoming in the modular construction is the stability issue of the structure, since the mechanical links between adjacent beams or columns from different modules are usually inadequate compared with traditional structures (Ha *et al*. 2016). Therefore, the rotational stiffness at the ends of a column in modular buildings or demountable buildings can also be weaker than that of a column in conventional structures (Wang *et al*. 2018). The insufficient connection stiffness will further induce larger slenderness of the structural columns in modular buildings. It is thus essential to implement stability analysis to evaluate the buckling performance and to identify the influential design factors for columns in modular structures.

As suggested in Fig. 5(a), as part of the complex boundary conditions for the connected columns, the presence of tenons will to some extent influence the buckling mode of the column, thereby the corresponding buckling load. Previous studies have indicated that the length and the stiffness of tenons at both ends have substantial influence on the buckling performance of a square hollow section (SHS) steel column (Deng *et al*. 2017). It should be noted that the previous research was based on a simplified boundary condition that both ends of the tenon-connected column are fixed. This would overestimate the genuine buckling strength of a modular column, since the rotation at tenon connection cannot be completely prevented in reality even though the modular frames might be braced and strengthened from lateral deflection. A schematic diagram of a tenon-connected column with rotational stiffness *k* at both ends are presented in Fig. 5(a). The rotational capacity of the tenon connection is related to the column-beam relative stiffness and the mechanical resistance against the shear slip between each pair of parallel components in the modular structure.

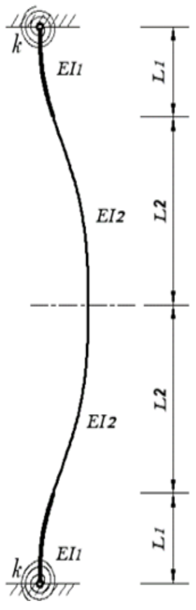

(a) Full length diagram of the column

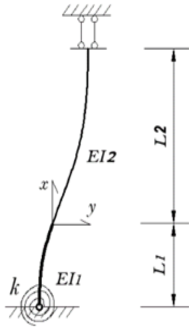

(b) Half length diagram of the column

Fig. 5 Diagram of a tenon-connected column with rotational stiffness *k* at the ends

Despite that concrete-filled steel tubes (CFST) have been used extensively in conventional building techniques due to their well-recognized excellent structural performances (Liew *et al*. 2012, Han *et al*. 2014, Ren *et al*. 2014, Hoang and Fehling 2017), current studies on the feasibility of applying composite structure into modular construction are yet very limited. Emerging researches (Liew *et al*. 2018) have recently been proposed on the potential practice of filling lightweight concrete with different grades in square hollow sections (SHS) to address the varied capacity requirements for columns in different layers of a modular structure. When CFST is adopted in the practice of modular construction, the concrete can be casted either in-situ or in factory depending on a few factors such as the construction period requirement, labor costs and crane capacities. Filling the concrete in factory can ensure its compactness and minimize the corresponding labor costs and construction time, whilst it is feasible only when sufficient crane capacities are in place. Conversely, on-site concrete casting is in advantage when the construction target period is more flexible.

This study thus intends to analyze the buckling performance of the tenon-connected columns, i.e., with SHS or CFST cross-sections, using both theoretical deductions and numerical simulations. The effects of

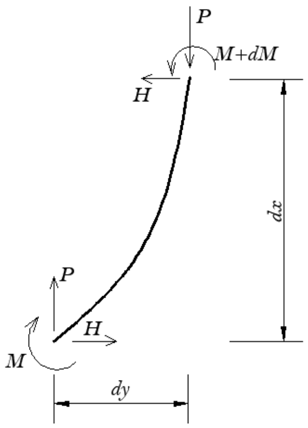

Fig. 6 Infinitesimal segment of a column with uniform section for buckling analysis

significant factors such as the tenon-length, the tenon-stiffness and the connection rotational stiffness will be evaluated. Design recommendations will then be proposed for this innovative tenon-connected inner connections in future modular construction.

2. The fourth-order deflection differential equations

According to the classic theory in structural stability (Chen and Liu 1987), the buckling modes of a column can be expressed as the multiple solutions for the fourth order deflection differential equation which can be solved with a set of specified boundary conditions. For tenon-connected columns in modular construction, specific adoption of this equation will be discussed to derive theoretical buckling loads for both SHS and CFST cross-sections. Based on the equilibrium analysis on any infinitesimal segment of a column as suggested in Fig. 6, the fourth order deflection differential equation can be generated as follows

$$EI\frac{d^4y}{dx^4}+P\frac{d^2y}{dx^2}=0 \tag{1}$$

Where x and y represent the longitudinal and transverse dimension of the column, respectively; EI stands for the bending stiffness of the column section; and P is the critical buckling load that satisfies the instantaneous balance conditions. Eq. (1) is suitable for any column that conform the classic Euler-Bernoulli beam assumptions, the general solution for this equation is expressed as follows

$$y=Asin(\alpha x)+Bcos(\alpha x)+Cx+D \tag{2}$$

Where $\alpha^2 = P$/EI. The buckling mode and the eigenvalue α can be obtained with corresponding boundary conditions of specific cases. Based on this classic theory, the buckling performance of tenon-connected SHS and CFST columns can then be evaluated with specified boundary conditions.

3. Stability analysis of a tenon-connected SHS column

3.1 Theoretical deduction of the characteristic equations

Compared to conventional structures, the innate slenderness of components in modular structures, the inevitable errors in fabrication and installation, and the slippage between adjacent beams and columns result in a large reduction in the rotational stiffness of the tenon connection. This further leads to a lower critical buckling load for the tenon-connected column. Therefore, the fixed-fixed end assumption tends to be aggressive and risky due to the neglection of the rotation flexibility at the connection. Traditionally, the stability design of a steel column in frames is conducted with special reference to the adjacent restraints by the beams and columns as presented in British Standards BS5950-1 (2000). However, the conventional approach cannot be effectively applied for this novel tenon-connected column in a modular structure due to the more complicated boundary conditions and the correlated influential factors stated above. Innovative stability analysis methods are thus developed in this section to deal with the specific issues in this kind of modular connection, i.e., the shear slip variation, the rotation stiffness variation and the tenon stiffness variation.

In a typical modular system, the cross-sectional dimensions of floor beams and ceiling beams are normally designed to be different to account for various design loads. The depth of the floor beam is usually around 50% greater than that of the ceiling beam (Lawson *et al*. 2014). When eight modules are connected together at the inner connection, the rotational stiffness at the top and bottom of a typical tenon-connected column is identical, as shown in Fig. 7, since both the floor beams and ceiling beams contribute to the restraining of potential relative rotation at the connections. As a result, the rotational stiffness of the

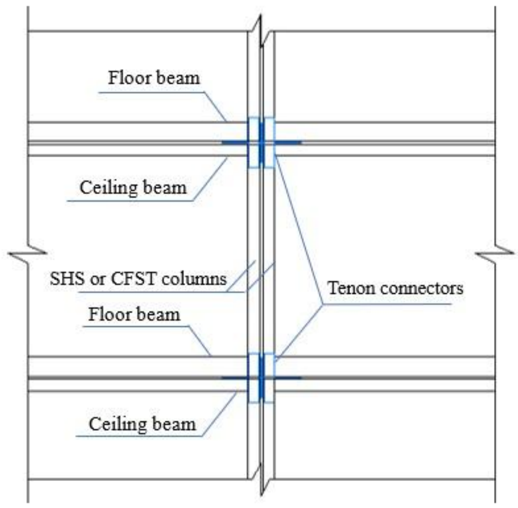

Fig. 7 Boundary conditions of the tenon-connected column in modular structure

top and bottom column ends is defined as the same value k, as shown in Fig. 5(a). According to symmetric consideration, only half of the column is analyzed hereby, with the simplification presented in Fig. 5(b). In Fig. 5, the column length and the bending stiffness of the tenon strengthened part and un-strengthened part are L_1, L_2 and EI_1, EI_2 respectively. Based on the general solution of the fourth order deflection differential equation demonstrated in Section 2

$$y_1 = A_1 sin(\alpha_1 x) + B_1 cos(\alpha_1 x) + C_1 x + D_1 \tag{3}$$

$$y_2 = A_2 sin(\alpha_2 x) + B_2 cos(\alpha_2 x) + C_2 x + D_2 \tag{4}$$

where y_1, y_2 represent the deformed shape of the tenon-strengthened bottom part and the top part of the half-column in Fig. 5(b), respectively. Eight pieces of boundary condition information are required to determine the final expression of the curves represented by Eqs. (3)-(4), sequentially the buckling load. Assume the rotation angle at the bottom end of the column to be θ, according to Euler-Bernoulli assumption, angle θ should satisfy

$$k\theta = M \tag{5}$$

$$k y_1^{'}(-L_1) = y_1^{''}(-L_1) EI_1 \tag{6}$$

Besides, the boundary conditions for the bottom part

$$y_1(-L_1) = 0 \tag{7}$$

$$y_1^{'}(-L_1) = \theta \tag{8}$$

Evaluating the mid-height symmetrical plane, the following two conditions are obtained

$$y_2^{'}(L_2) = 0 \tag{9}$$

$$y_2^{'''}(L_2) = 0 \tag{10}$$

Furthermore, at the intersection of the tenon-strengthened part and the part without tenon strengthening, four continuity conditions are applied

$$y_1(0) = y_2(0) \tag{11}$$

$$y_1^{'}(0) = y_2^{'}(0) \tag{12}$$

$$EI_1 y_1^{''}(0) = EI_2 y_2^{''}(0) \tag{13}$$

$$EI_1 y_1^{'''}(0) = EI_2 y_2^{'''}(0) \tag{14}$$

Therefore, nine equations are obtained from Eqs. (6)-(14) for solving nine unknowns from A_1 to D_2 plus θ, the simultaneous equation is thus solvable. From Eqs. (10)-(14), five conditions can be easily achieved, i.e., $D_1 = D_2$, $C_1 = C_2$, $C_2 = 0$, $B_1 = B_2$, $A_1\alpha_1 = A_2\alpha_2$. Substituting these conditions into Eqs. (6)-(9), nine unknowns could be simplified to three after mathematical rearrangement

$$-A_2 \frac{\alpha_2}{\alpha_1} sin(\alpha_1 L_1) + B_2 cos(\alpha_1 L_1) + D_2 = 0 \tag{15}$$

$$A_2 \alpha_2 \, cos(\alpha_2 L_2) - B_2 \alpha_2 \, sin(\alpha_2 L_2) = 0 \tag{16}$$

$$\begin{aligned} &\left[k\alpha_2 \, cos(\alpha_1 L_1) - P\frac{\alpha_2}{\alpha_1} sin(\alpha_1 L_1)\right] A_2 \\ &+ [k\alpha_1 \, sin(\alpha_1 L_1) + P cos(\alpha_1 L_1)] B_2 = 0 \end{aligned} \tag{17}$$

To achieve nontrivial solution for the above set of simultaneous equations, the determinant of the following matrix should be zero

$$\begin{vmatrix} -\frac{\alpha_2}{\alpha_1} sin(\alpha_1 L_1) & cos(\alpha_1 L_1) & 1 \\ \alpha_2 \, cos(\alpha_2 L_2) & -\alpha_2 \, sin(\alpha_2 L_2) & 0 \\ k\alpha_2 \, cos(\alpha_1 L_1) - P\frac{\alpha_2}{\alpha_1} sin(\alpha_1 L_1) & k\alpha_1 \, sin(\alpha_1 L_1) + P cos(\alpha_1 L_1) & 0 \end{vmatrix} = 0 \tag{18}$$

Where

$$P = \alpha_1^2 EI_1 = \alpha_2^2 EI_2 \tag{19}$$

Solving the determinant, the characteristic equation is derived as follows

$$\begin{aligned} &k\alpha_1\alpha_2 \sin(\alpha_1 L_1) \, cos(\alpha_2 L_2) \\ &+ P\alpha_2 \, cos(\alpha_1 L_1) \, cos(\alpha_2 L_2) \\ &+ k\alpha_2^2 \, cos(\alpha_1 L_1) sin(\alpha_2 L_2) \\ &- P\frac{\alpha_2^2}{\alpha_1} sin(\alpha_1 L_1) \sin(\alpha_2 L_2) = 0 \end{aligned} \tag{20}$$

Eq. (20) could be further simplified to a compact form as Eq. (21)

$$\begin{aligned} &\frac{k\alpha_1}{P} \tan(\alpha_1 L_1) + 1 + \frac{k\alpha_2}{P} \tan(\alpha_2 L_2) \\ &- \frac{\alpha_2}{\alpha_1} \tan(\alpha_1 L_1) \tan(\alpha_2 L_2) = 0 \end{aligned} \tag{21}$$

Eq. (21) is the general characteristic equation for determining the critical buckling load of a tenon-connected column with rotational stiffness k at both ends. As can be found, Eq. (21) contains three non-dimensional variables: the relative bending stiffness ratio m, the relative length ratio n and the relative rotational stiffness ratio λ defined as Eqs. (22)-(24). Thus, the original Eq. (21) can be rewritten as Eq. (25), which contains only one unknown $\alpha_1 L_1$ and is solvable mathematically when the values for the above defined factors m, n and λ are determined.

$$m = \frac{EI_1}{EI_2} = \frac{\alpha_2^2}{\alpha_1^2} \tag{22}$$

$$n = \frac{L_1}{L_2} \tag{23}$$

$$\lambda = \frac{k\alpha_1}{P} \tag{24}$$

$$\begin{aligned} &\lambda \, tan(\alpha_1 L_1) + 1 + \lambda\sqrt{m} \, tan\left(\frac{\sqrt{m}}{n}\alpha_1 L_1\right) \\ &- \sqrt{m} \, tan(\alpha_1 L_1) \, tan\left(\frac{\sqrt{m}}{n}\alpha_1 L_1\right) = 0 \end{aligned} \tag{25}$$

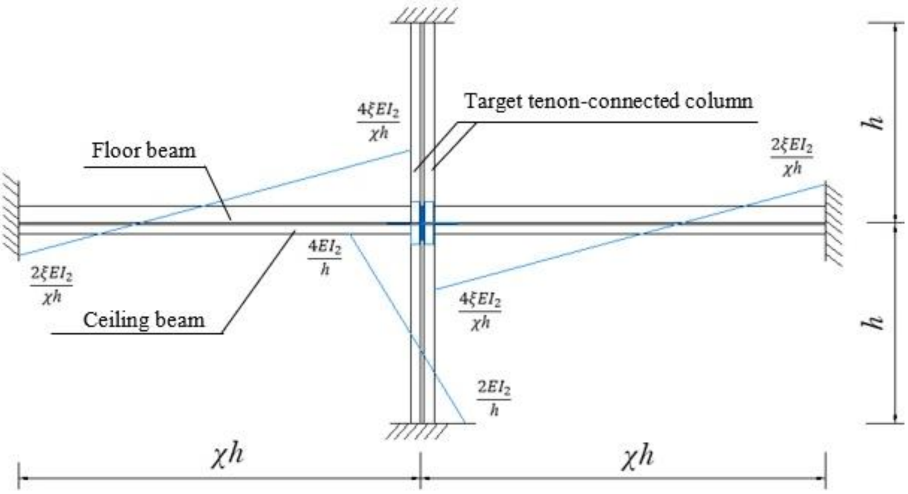

(a) Rotational stiffness of each connected component

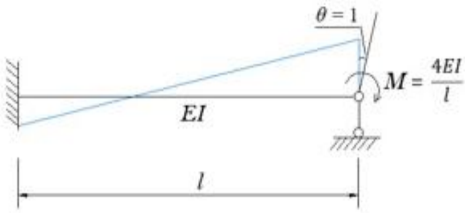

(b) Rotational stiffness of a component with uniform cross-section and fixed far end

Fig. 8 Rotational stiffness of the components framed to the tenon connection

As can be seen, if no contributions of the tenons are taken into account, i.e., where m = 1 and n = 0, the characteristic Eq. (25) can be simplified and a more precise effective length coefficient can be obtained, which is consistent with the traditional method in British Standards BS5950-1 (2000).

3.2 Interval analysis of relative rotational stiffness ratio λ

Three non-dimensional variables m, n and λ have been proposed in Eqs. (22)-(24). The relative bending stiffness ratio m and relative length ratio n represent the ratio of the flexural stiffness and the segment length between the tenon-strengthened column segment and the segment with no tenon inside, as shown in Fig. 5. For the defined relative rotational stiffness ratio λ, α_1 and P are correlated and rotational stiffness k relies on the geometric and structural features of module units. Hence, λ is a complex factor affected by the overall mechanism of the modular connections. In-depth evaluation of the factor λ needs to be fully understood so that the transcendental Eq. (25) can be solved with rational input values. In view of the variability for the composing parameters in the expression of λ, the variable range of λ in practice need to be investigated coordinately through comprehensive interval analysis. The following assumptions are adopted in Section 3.2 for the interval analysis for the ease of theoretical deduction: (1) The geometric dimensions and material properties of all adjacent modules are identical; (2) The far ends of the vertical and horizontal components framed into the tenon connection are assumed to be rigid, as shown in Fig. 8(a); (3) The cross-sectional dimensions of the ceiling and floor beams are chosen as identical to that of a single tenon-connected column; (4) The benefits brought by the tenon to the column's bending and rotational stiffness in the tenon-strengthened segment is neglected. The following sections aim to discuss the interval of factor λ and its corresponding influence to the tenon-connected column.

3.2.1 The interval of geometric uncertainty factor χ

The overall height and length of each module are defined as h and χh respectively. In general applications, the length of a module is ranging from 6 to 12 m (Lawson *et al*. 2014), with the typical floor height around 3 m, leaving the interval for χ as

$$\chi \in [2,4] \tag{26}$$

3.2.2 The interval of shear slip uncertainty factor ξ

In typical practice, linking bolts are adopted to connect the adjacent floor beams and ceiling beams so that to achieve a higher sectional bending stiffness. On the contrary, there is hardly any connection along the column length of the adjacent columns from different modules due to their design purpose of resisting the vertical loads (Monash University 2017). Based on the different linking patterns between parallel columns and beams, there is large variation on the bending stiffness of different components. Various types of inter-unit connections could induce full slip, partial slip and non-slip mechanical effects based on the shear actions at the interface between adjacent beams or columns. The bending stiffness of the columns and beams with different sectional configurations are presented in

Table 1 Bending stiffness of typical cross sections under different conditions

Loading scenario	Column full slip	Beam		
		Full slip	Partial slip	Non-slip
Sectional view	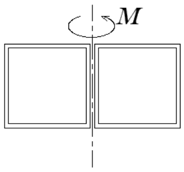	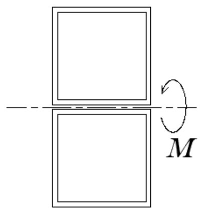	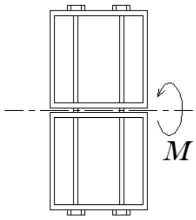	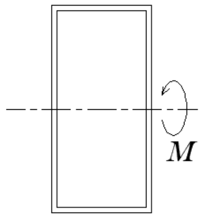
Bending stiffness	$2\times\frac{1}{12}(D^4-d^4)E = EI_2$	$2\times\frac{1}{12}(D^4-d^4)E = EI_2$	$2\times\frac{\xi}{12}(D^4-d^4)E = \xi EI_2$	$2\times\frac{4}{12}(D^4-d^4)E = 4EI_2$

Table 1, where D and d represent the external and internal side widths of a SHS component.

As shown in Table 1, the minimum sectional bending stiffness is achieved when full slip occurs between adjacent SHS sections, which equals twice the bending stiffness of the original single column. For the maximum scenario, no slip between adjacent sections exists, i.e., the shear linking bolts are strong enough to enable the adjacent sections to function as an integrate in resisting external bending moment. In this case, the bending stiffness can be calculated as

$$EI = \frac{1}{12}\times[(2D)^3\times D-(2d)^3\times d]E = 2\times\frac{4}{12}(D^4-d^4)E = 4EI_2 \quad (27)$$

The bending stiffness of a pair of beams is considered to be ξEI_2 under practical conditions, where ξ is the bending stiffness modification factor against the reference value EI_2 from a pair of parallel columns or full slip beams. Since the real circumstance lies in between the full slip and non-slip scenario, the interval of ξ could be determined as

$$\xi\epsilon[1,4] \quad (28)$$

3.2.3 The expression of rotational stiffness k

As illustrated in Fig. 8(a), the rotational stiffness k of a tenon connection is affected by the bending stiffness of each pair of components framed into it except for the columns under buckling analysis. It is reasonable to neglect the bending stiffness of the target analyzed components since

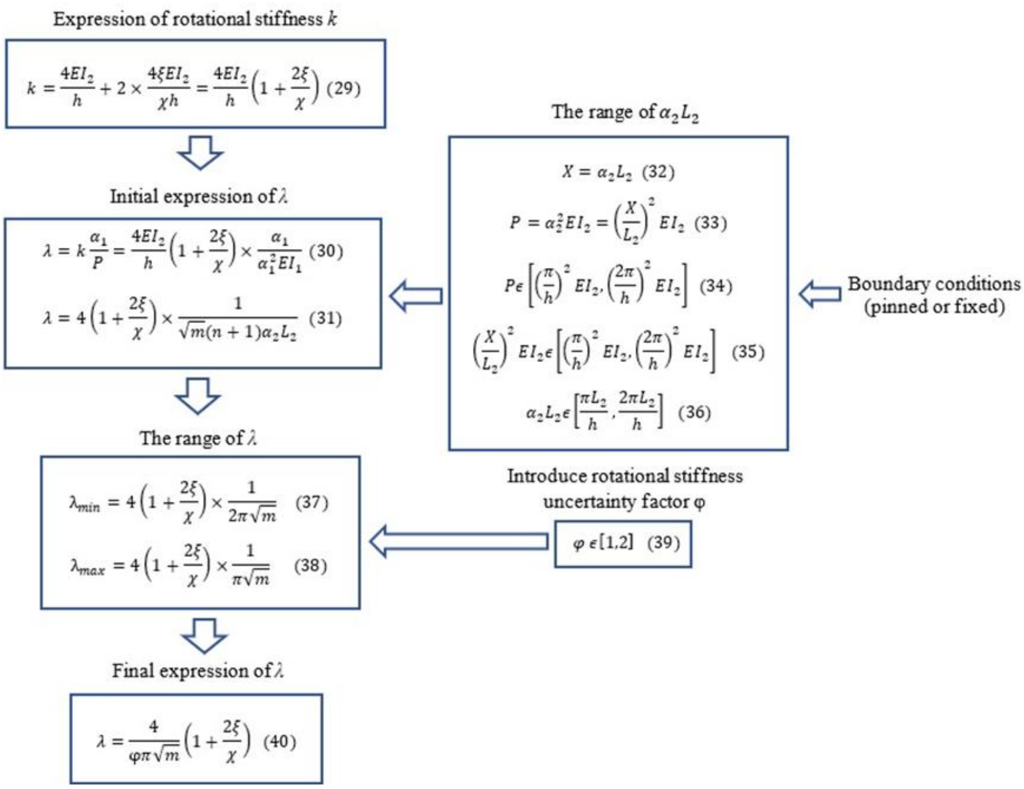

Fig. 9 The deduction of relative rotational stiffness ratio λ

the target column cannot prohibit itself from further deflection when its buckling strength is reached. Hence, the rotational stiffness k shown in Fig. 8(a) is contributed from four horizontal beams (paralleled ceiling and floor beams) and two vertical columns. In the light of elastic angular-displacement equation, the required moment to incur a unit angular rotation at the end of a component is presented in Fig. 8(b). Since the interval of a component's length and its bending stiffness has been characterized by χ and ξ as denoted above, the rotational stiffness at the connection of a group of modules could be expressed as

$$k = \frac{4EI_2}{h} + 2 \times \frac{4\xi EI_2}{\chi h} = \frac{4EI_2}{h}\left(1 + \frac{2\xi}{\chi}\right) \quad (29)$$

3.2.4 The interval of rotational stiffness uncertainty factor φ

Fig. 9 shows the procedures to derive the final expression of the relative rotational stiffness ratio λ from the initial expression of k in Eq. (29). The critical buckling load of a tenon-connected column reaches its minimum and maximum value when its two ends are both pinned and both fixed respectively. By introducing the rotational stiffness uncertainty factor φ, the final expression of λ is expressed as

$$\lambda = \frac{4}{\varphi\pi\sqrt{m}}\left(1 + \frac{2\xi}{\chi}\right) \quad (30)$$

As can be seen, there are four interval factors χ, ξ, φ and m included in the general formula Eq. (40), representing the geometry uncertainty, shear slip uncertainty, rotational stiffness uncertainly and tenon stiffness uncertainty of a typical tenon inner connection in a modular structure.

3.2.5 The interval of tenon stiffness uncertainty factor m

As can be deduced, if the dimension of the internal tenon section is of similar geometry and material property as the external SHS section, the relative bending stiffness ratio m is around 2. However, a much larger bending stiffness of the tenon can be reached by increasing the wall thickness. For conservative reasons, the range of the relative bending stiffness ratio m is taken as 1 to 10 as follows

$$m\epsilon[1,10] \quad (41)$$

3.2.6 The interval of relative rotational stiffness ratio λ

According to Eqs. (26), (28), (39) and (41), the variation interval for these four factors have been determined as $\chi\epsilon[2,4]$, $\xi\epsilon[1,4]$, $\varphi\epsilon[1,2]$ and $m\epsilon[1,10]$. Therefore, the interval for λ could be determined quantitatively.

$$\lambda_{min} = f(\chi,\xi,\varphi,m) = f(4,1,2,10) = \frac{3}{\pi\sqrt{10}} \approx 0.302 \quad (42)$$

$$\lambda_{max} = f(\chi,\xi,\varphi,m) = f(2,4,1,1) = \frac{20}{\pi} \approx 6.366 \quad (43)$$

Thus

$$\lambda\epsilon[0.302, 6.366] \quad (44)$$

Taking $\lambda \in [0,6]$ as the basic interval to solve the characteristic Eq. (25) under additional conditions m = 2.0 and n = 0.2, the transcendental equation can then be solved mathematically. Table 2 presents the buckling load of the tenon-connected column P_m the rotational stiffness k and the effective length coefficient μ under different λ values. The relation of μ and λ are illustrated in Fig. 10, from which a conceptual conclusion could be drawn: when λ is ranging from 0 to 3.0, the effective length coefficient μ is highly related to λ; however, when λ is larger than 3.0, the value of μ is less sensitive to further increase of λ. Considering the actual effective influence interval of λ, the variation domain of λ could be remodified as $\lambda \in [0,3]$ for better depicting the interdependent relation between the relative rotational stiffness ratio λ and the effective length coefficient μ.

It should be noted that geometric imperfection is not considered in the theoretical buckling deduction for the tenon-connected column due to the lack of compact solution for the buckling capacity of an imperfect column through classical analytical method. Instead, numerical methods

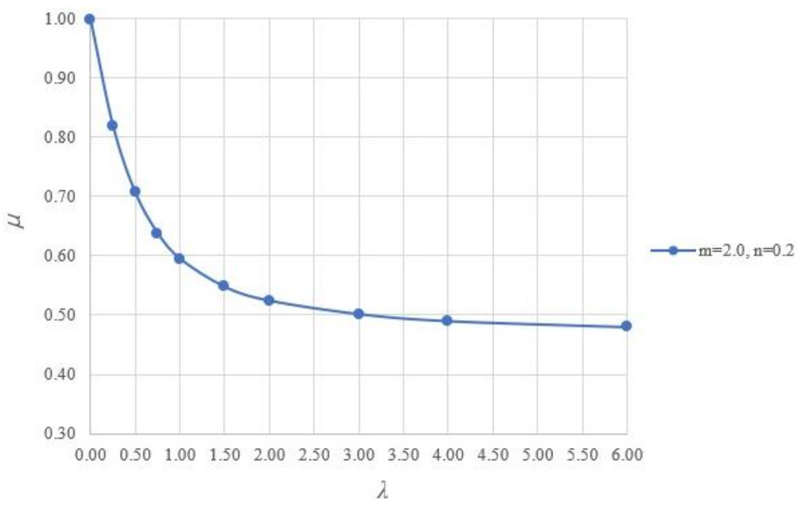

Fig. 10 The relationship between μ and λ when m = 2 and n = 0.2

Table 2 The relation between factors μ and λ

λ	P_m (N)	P_o (N)	k (Nm)	μ
0.00	16,964	16,895	0	0.9980
0.25	25,181	16,895	6,963,806	0.8191
0.50	33,842	16,895	16,146,169	0.7066
0.75	41,462	16,895	26,807,571	0.6383
1.00	47,684	16,895	38,331,745	0.5952
1.50	56,323	16,895	62,489,372	0.5477
2.00	61,433	16,895	87,016,759	0.5244
3.00	67,129	16,895	136,441,292	0.5017
4.00	70,443	16,895	186,358,838	0.4897
6.00	73,456	16,895	285,454,411	0.4796

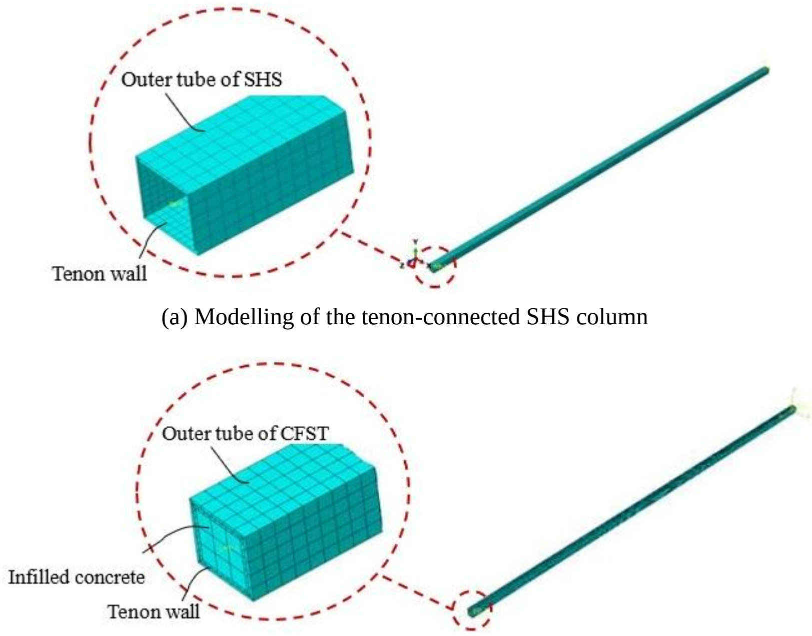

(a) Modelling of the tenon-connected SHS column

(b) Modelling of the tenon-connected CFST column

Fig. 11 General view of the numerical modelling for tenon-connected columns in ABAQUS

with adequate iterations in the loading process can be applied to approach the nonlinear buckling behaviour. The geometric imperfection can also be accounted for through the introduction of amplification factors against the buckling capacity of an ideally perfect column, as suggested in AS4100 (1998).

3.3 Numerical validation of the characteristic equations

The finite element analysis (FEA) program package ABAQUS is adopted in this study to provide numerical validation for the deduced characteristic equations. It is worth mentioning that the geometric imperfection has been correspondingly disregarded in the numerical modelling in order to be consistent with the theoretical part and provide objective validation for the theoretical results. Since the reasonable interval of λ has been determined in Section 3.2, the characteristic Eq. (25) is then solved mathematically for the buckling strength of a tenon-connected column. According to Eq. (24), the expression of k could be written as

$$k = \frac{\lambda P}{\alpha_1} \tag{45}$$

The transcendental Eq. (25) about $\alpha_1 L_1$ has a number of theoretical solutions, while the minimum positive solution reflects the real buckling performance. After the determination of $\alpha_1 L_1$, the rotational stiffness k can be derived as well based on Eq. (45) and then be specified in the ABAQUS modelling. In summary, the k, m and n values specified or obtained in theoretical trials are adopted in the numerical modelling as well to determine the buckling load of a tenon-connected column, so that the feasibility of the characteristic equations can be evaluated.

To ensure that the column would buckle before yield,

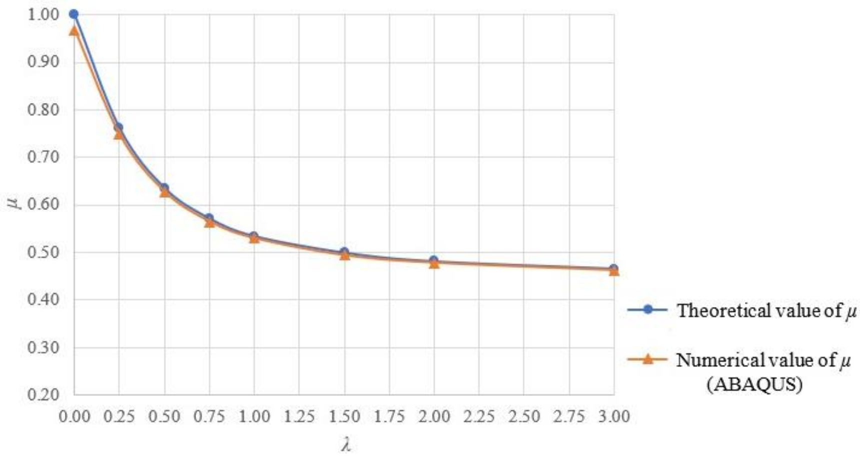

Fig. 12 Comparison between the analyzed and theoretical values for effective length coefficient μ

a 40×40×2 mm steel section and a 36×36×2 mm tenon section are selected to simulate the elastic buckling behavior of a 3 m long SHS column. Both the external steel tube and the internal tenons are modelled using 4-node shell elements with full integration in ABAQUS with linear-elastic material properties. The external steel tube is assigned with 210,000 MPa for elastic modulus and 0.33 for Poisson's ratio. The elastic modulus for the internal tenon is adjusted to a point where the relative bending stiffness ratio m is 4.0, as calculated by Eq. (22). The internal tenons are attached to the external steel tube with normal contact restriction and tangential friction with a friction coefficient of 0.6. The length ratio n is defined as 0.2 in the modelling, as calculated by Eq. (23). A general view of the FEA modelling for a tenon-connected SHS column is presented in Fig. 11(a).

The effective length coefficient μ calculated from both theoretical deduction and ABAQUS buckling analysis are compared in Fig. 12. As can be seen, the numerical values derived from ABAQUS modelling closely match those deducted from Eq. (25) with λ ranging from 0 to 3.0. The error between the theoretical and numerical solutions is generally less than 3%, indicating the feasibility of the deduced characteristic equations.

4. Stability analysis of a tenon-connected CFST column

4.1 Theoretical deduction of the characteristic equations

Filling the hollow steel column with concrete has proved to be an effective way to greatly enhance the strength, stiffness and robustness behavior of the structural columns (Lam and Williams 2004, Han *et al*. 2014). It is expected that the adoption of CFST columns has great potential to be explored in modular construction. This section thus focuses on the global stability analysis of a tenon-connected CFST column with square section. In terms of local buckling, the performance of CFST column is expected to be much better compared with SHS column due to the internal support from the infilled concrete. However, global buckling can still occur for a relative slender column commonly seen in modular units.

Fig. 13(a) illustrates the geometric features and the corresponding material modules for a square CFST cross-section. According to elasticity analysis, the concrete modulus E_c is regarded effective across the entire section under compressive load when the column reaches its buckling strength, attributing to the confinement of the outer steel tube. With D and d defined as the external and internal side width of the outer steel tube, the bending stiffness of the entire composite section can be calculated as

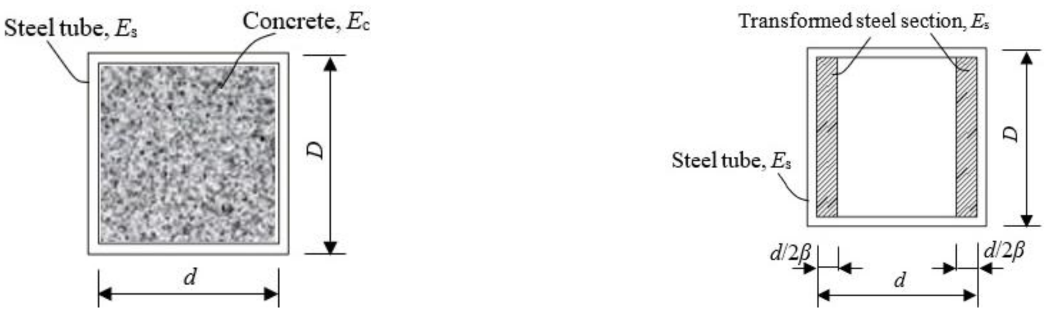

(a) Original square CFST cross-section (b) Transformed effective steel section

Fig. 13 The effective section transformation method for CFST cross-sections

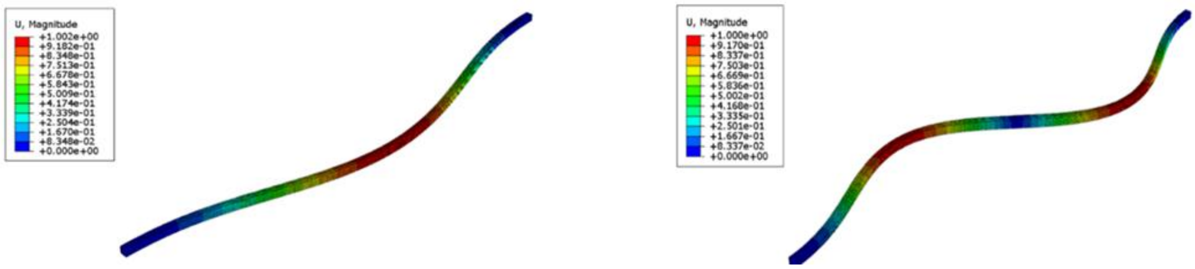

(a) The 1st buckling mode (b) The 3rd buckling mode

Fig. 14 The analyzed buckling modes for tenon-connected columns

$EI = E_s \times \frac{1}{12}(D^4 - d^4) + E_c \times \frac{1}{12}d^4$. Introducing an additional factor $\beta = E_s/E_c$ as the section modulus ratio, the bending stiffness of the entire section could be calculated as follow

$$\begin{aligned} EI &= E_s \times \frac{1}{12}(D^4 - d^4) + \frac{E_s}{\beta} \times \frac{1}{12}d^4 \\ &= E_s \times \frac{1}{12}(D^4 - d^4) + E_s \times \frac{1}{12}d^3 \times \frac{d}{\beta} \end{aligned} \tag{46}$$

A transformed effective steel section is used to replace the original CFST section in the theoretical deduction, as shown in Fig. 13(b). As shown in the figure, the transformed effective section is divided into three parts, i.e., the original steel section (double layered at the end of a column to account for the tenon while single layered in the middle section), the effective steel section part transformed from the core concrete, and the hollow part in the middle due to the relatively lower elastic modulus of concrete material compared with steel.

These characteristics have been reflected in Eq. (46) as well. As shown in Eq. (46), the effective steel section transformed from the concrete is deemed as an equivalent section with a height of d and a width of d/β and is equally divided into two parts for a symmetric configuration, where d/β is the equivalent width. Using this transformation method, the concrete infill with any grade can be replaced by additional steel plates to comprise an equivalent section with single steel material, so that the characteristic equation explained in Section 3 is still valid for the stability analysis.

4.2 Numerical validation of the characteristic equations

FEA modelling using ABAQUS is also conducted for tenon-connected CFST column to validate the theory of section transformation. The general view of the established numerical modelling for tenon-connected CFST column is shown in Fig. 11(b), where the elastic material property and element meshing of steel tube and tenon wall are the same with what described in Section 3.2. As mentioned above, the potential geometric imperfection has been neglected in the numerical modelling to be consistent with the theoretical counterpart. As a matter of fact, it has been reported that the concrete infill in CFST can effectively reduce the impact of imperfection on a tubular column (Han *et al*. 2014). The approach to consider geometric imperfection in the FEA simulation of slender CFST columns has been presented in An *et al*. (2012).

In the FEA modelling, the elastic modulus for concrete and steel are defined as 30,100 MPa and 210,000 MPa, respectively, resulting in a modulus ratio β of 6.98. For the column end segment, the sectional components include 40×40×2 mm outer steel section, 36×36×2 mm tenon wall ection, and 32×32 mm core concrete section. For the un-strengthened column segment in the middle, the sectional components include 40×40×2 mm outer steel section and 36×36 mm core concrete section. The length ratio n (L_1/L_2) is preset as 0.2. The contact between the core concrete and the outer steel tube is simulated between two matching surfaces, where separation is allowed while penetration is restrained. Interface properties with hard contact in the normal direction and a Coulomb friction model in the tangential direction is defined between the steel and concrete, with the friction coefficient defined as 0.6 (Han *et al*. 2014).

For the above tenon-connected CFST column described in the simulation, according to Eq. (46), the theoretical bending stiffness of the transformed section in the middle and at the end of the column can be expressed as follows

$$\begin{aligned} EI_{mid} &= 210000 \times \frac{1}{12}\left[40^4 - 36^3\left(36 - \frac{36}{6.98}\right)\right] \\ &= 1.962 \times 10^{10} \text{ MPa} \end{aligned} \tag{47}$$

$$\begin{aligned} EI_{end} &= 210000 \times \frac{1}{12}\left[40^4 - 32^3\left(32 - \frac{32}{6.98}\right)\right] \\ &= 2.908 \times 10^{10} \text{ MPa} \end{aligned} \tag{48}$$

Hence, the relative bending stiffness ratio m is calculated as

$$m = \frac{EI_1}{EI_2} = \frac{EI_{end}}{EI_{mid}} = 1.482 \tag{49}$$

The buckling behavior of the described tenon-connected CFST column is evaluated through ABAQUS modelling. Four eigenvalues of the CFST column are extracted, with the corresponding buckling modes displayed in Fig. 14. According to the numerical results, the 1st buckling mode corresponds to the most critical buckling load, which is 96,168 N. For comparison, the theoretical critical buckling load of a standard Euler column without tenon P_o is calculated as Eq (50).

$$P_o = \frac{\pi^2 \times EI_{\mathrm{mid}}}{L^2} = \frac{\pi^2 \times 1.962 \times 10^{10}}{3000^2} = 21.52\ kN \tag{50}$$

Thus, the effective length coefficient μ from numerical analysis is calculated as

$$\mu_{\text{Numerical}} = \sqrt{\frac{21.52}{96.17}} = 0.473 \tag{51}$$

Theoretically, provided that both ends are fixed, i.e., the rotational stiffness k approaches infinite, Eq. (25) can be further simplified as Eq. (52) for the calculation of the theoretical buckling load. After trial and errors procedures, the equation was found to be valid when eigenvalue $\alpha_1 L_1$ is 0.453. By solving Eq. (52), the theoretical buckling load P_{m} and the theoretical effective length coefficient μ for the tenon-connected CFST column can be calculated as Eqs. (53)-(54), respectively. By comparing the effective length coefficient μ obtained from both numerical and theoretical methods, the difference factor δ_{A} is found in Eq. (55).

$$\tan(\alpha_1 L_1) + \sqrt{m}\, tan\left(\frac{\sqrt{m}}{n}\alpha_1 L_1\right) = 0 \tag{52}$$

$$\begin{aligned} P_{\mathrm{m}} &= \left(\frac{\alpha_1 L_1}{L_1}\right)^2 EI_1 \\ &= \left(\frac{0.453}{250}\right)^2 \times 2.908 \times 10^{10} = 95.48\ kN \end{aligned} \tag{53}$$

$$\mu_{Theoretical} = \sqrt{\frac{P_m}{P_o}} = 0.475 \tag{54}$$

$$\begin{aligned} \delta_A &= \left|\frac{\mu_{Numerical} - \mu_{Theoretical}}{\mu_{Theoretical}}\right| \\ &= \left|\frac{0.473 - 0.475}{0.475}\right| = 0.4\% \end{aligned} \tag{55}$$

The difference between the effective length coefficients μ for tenon-connected CFST column calculated from theoretical deduction and that obtained from FEA numerical modelling is only 0.4%, proving the feasibility of both the theoretical deduction and numerical modelling. Moreover, the excellent agreement also indicates that the above mentioned effective section transformation method can successfully characterize the buckling performance of a tenon-connected CFST column. Consequently, for stability analysis of a typical tenon-connected column in modular construction, the global buckling behavior is governed by the characteristic Eq. (25) regardless of the sectional configuration.

5. Analysis and discussions

The deduced characteristic Eq. (25) has been proved to be applicable in the buckling analysis for both tenon-connected SHS and CFST columns in modular construction. Further discussions on Eq. (25) are conducted to evaluate the influence of significant structural factors including the relative bending stiffness ratio m, the relative length ratio n and the relative rotational stiffness ratio λ as defined in Eqs. (22)-(24), respectively. In the following sessions, the

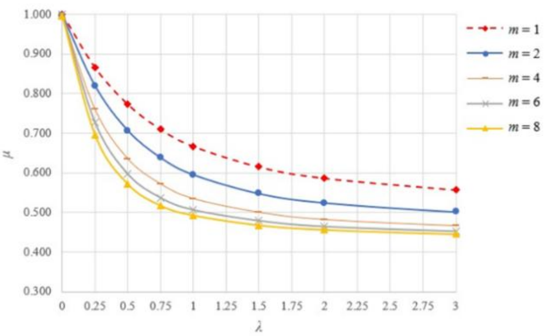

(a) Variation of relative bending stiffness ratio m

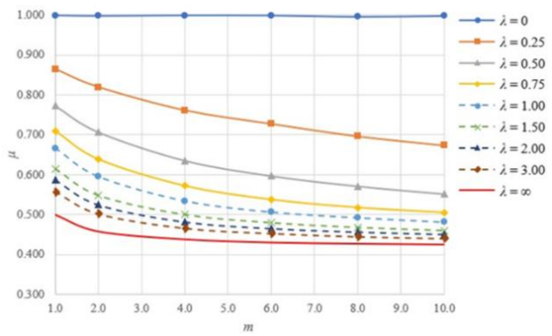

(b) Variation of relative rotational stiffness ratio λ

Fig. 15 The effective length coefficient μ under different m and λ values when n = 0.2

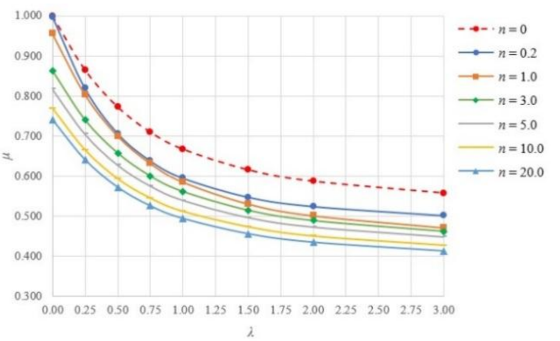

(a) Variation of relative length ratio n

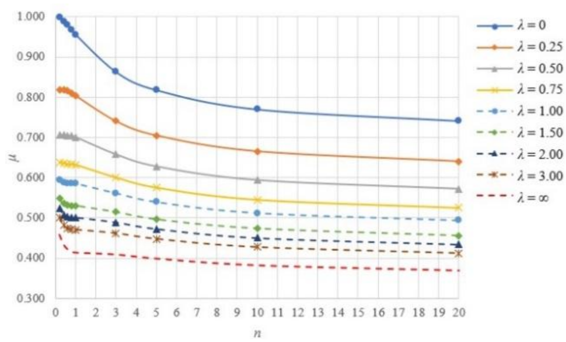

(b) Variation of relative rotational stiffness ratio λ

Fig. 16 The effective length coefficient μ under different n and λ values when m = 2.0

Table 3 The changing rules of factors μ, λ and m under various cases

Cases			Results		
With fixed n (Relative length ratio)	λ (Relative rotational stiffness ratio)	↑	μ (Effective length coefficient)	↓	The change of μ is less sensitive when λ gets larger
	m (Relative bending stiffness ratio)	↑		→	For pinned-pinned boundary conditions
				↓	For other boundary conditions
With fixed m (Relative bending stiffness ratio)	λ (Relative rotational stiffness ratio)	↑		↓	The change of μ is less sensitive when λ or n gets larger
	n (Relative length ratio)	↑			

relative length ratio n and the relative bending stiffness ratio m are successively fixed for better demonstrating the relationship among the buckling behavior, i.e., the effective length coefficient μ, and the rest two factors.

5.1 The relation among μ, λ and m under fixed n

Under a fixed relative length ratio n = 0.2, the relationship between the effective length coefficient μ and the relative rotational stiffness ratio λ as well as the relative bending stiffness ratio m are presented in Figs. 15(a)-(b). The summarization of the changing rules of these factors are listed in Table 3 as well. The following discussions can be conducted based on the results presented in Fig. 15 and Table 3

- The effective length coefficient μ decreases with the increase of the rotational stiffness k and the relative rotational stiffness ratio λ, indicating that increasing the rotational stiffness at both ends of a tenon-connected column can lead to a higher buckling load of the column.
- When the rotational stiffness ratio λ is larger than a specific criterion, its buckling load is less sensitive to the further increase of the rotational stiffness k. With λ > 3, the effective length coefficient μ under various m values is close to its ultimate value when λ approaches infinite, i.e., the fixed-fixed boundary conditions for the column.
- The effective length coefficient μ decreases with the increase of the tenon stiffness except for a simply supported column, thus resulting in a higher critical buckling load for the tenon-connected column.
- With the rotational stiffness ratio λ = 0, the effective length coefficient μ remains to be around 1.0 regardless of the variation of m. The effect of tenon stiffness on the effective length of a simply supported column is neglectable when the relative length ratio n is relatively small.
- The red dash line in Fig. 15(a) reflects the effective length coefficient μ of a column without tenons, which corresponds to the upper limit of the column effective length and demonstrates the benefits brought by the tenons.
- As can be seen in Fig. 15(b), the effective length calculated for a fixed-fixed column, i.e., the solid line with red colour, is much smaller than that of the actual scenario with the potential rotation at column ends considered. This proves that the assumption of fixed-fixed boundary condition results in over-estimation for the critical buckling load of the tenon-connected column in modular structures. It is necessary to take the rotational stiffness of the tenon connections into consideration for safety reasons.

5.2 The relation among μ, λ and n under fixed m

Under a fixed relative bending stiffness ratio m = 2.0, the relationship between the effective length coefficient μ and the relative rotational stiffness ratio λ as well as the relative length ratio n are presented in Figs. 16(a)-(b). The summarization of the changing rules of these factors are listed in Table 3 as well. The following discussions can be conducted based on the results presented in Fig. 16 and Table 3,

- The effective length coefficient μ decreases with the increase of the relative length ratio n, indicating that increasing the length of the tenon can bring about a higher critical buckling load of the tenon-connected column. The red dash line in Fig. 16(a) presents the upper bound of μ when the tenon length approaches infinitesimal, which helps demonstrate the contribution of the tenon in preventing immature buckling of the column.
- The effective length coefficient μ decreases gradually when the relative rotational stiffness ratio λ or the relative length ratio n is higher than a specific threshold. Afterwards, the buckling load of a tenon-connected column is less sensitive to the further increment of λ or n.
- The effective length based on that the assumption of fixed-fixed boundary condition, i.e., the red line in Fig. 16(b), is much smaller than the actual scenario with the potential rotation of column ends considered. This again demonstrates that the actual rotational stiffness of the tenon connection needs to

be accounted for in the stability analysis of tenon-connected columns in modular construction.

6. Conclusions

The research work reported in this current paper allows the following conclusions to be drawn,

- The application of the novel inner connections incorporating tenons and gusset plates can effectively solve the internal tying issues of modular construction. Stability analysis of a tenon-connected SHS column was conducted through theoretical evaluation on the characteristic fourth order differential equations. The assumption of fixed-fixed boundary condition is proved to induce risk in the buckling analysis, indicating that the rotational capacity of the tenon connection needs to be taken into consideration in the stability design of tenon-connected columns in modular construction.
- The feasibility of using CFST columns in modular construction to enhance the stability is validated through the theoretical study. It has been proved that the effective section transformation method can successfully predict the global buckling behavior of a CFST column, which reflects the universal applicability of the characteristic equations for tenon-connected columns.
- Numerical analysis on the stability performance of tenon-connected SHS and CFST column has been developed using finite element analysis method. The effective buckling lengths calculated from both theoretical deduction and ABAQUS buckling analysis agree well, indicating the effectiveness of both the theoretical equations and the numerical modelling.
- The effects of significant factors such as the tenon-length, the tenon-stiffness and the connection rotational stiffness on the buckling behavior of tenon-connected SHS and CFST columns are evaluated. The changing rules of the effective length coefficient μ against the relative bending stiffness ratio m, the relative length ratio n and the relative rotational stiffness ratio λ are presented and discussed, as summarized in Section 5.

It should be noted that, although this study has presented a comprehensive theoretical and numerical discussion on the buckling performance of tenon-connected SHS and CFST columns in modular construction, further studies on the strength, seismic behavior and long-term behavior of such innovative structural columns and connections are needed in the future to ensure their safe and effective application in practice.

Acknowledgments

The research reported in this paper is part of the Early Career Research Grant of Faculty of Engineering and IT, The University of Sydney. The financial support is highly appreciated.

References

An, Y.F., Han, L.H. and Zhao, X.L. (2012), “Behaviour and design calculations on very slender thin-walled CFST columns”, *Thin-Wall. Struct.*, **53**, 161-175.

Annan, C.D. (2008), “Applicability of traditional design procedures to modular steel buildings”, Ph.D. Dissertation; The University of Western Ontario, London, ON, Canada.

AS4100 (1998), Australian Standards Steel Structures, Standards Australia Limited; Sydney, Australia.

BS5950 (2000), Structural use of steelwork in building. Part 1: Code of practice for design - Rolled and welded sections; London, UK.

Chen, W.E. and Liu, E.M. (1987), *Structural Stability: Theory and Implementation*, (1st Ed.), Prentice Hall, Upper Saddle River, NJ, USA.

Chen, Z.H., Liu, J.D. and Yu, Y.J. (2017a), “Experimental study on interior connections in modular steel buildings”, *Eng. Struct.*, **147**, 625-638.

Chen, Z.H., Liu, J.D., Yu, Y.J., Zhou, C.H. and Yan R.J. (2017b), “Experimental study of an innovative modular steel building connection”, *J. Constr. Steel Res.*, **139**, 69-82.

Choi, K.S. and Kim, H.J. (2014), “Analytical models of beam-column joints in a unit modular frame”, *J. Computat. Struct. Eng. Inst. Korea*, **27**(6), 663-672.

Chua, Y.S., Liew, J.Y.R. and Pang, S.D. (2018), “Robustness of prefabricated prefinished volumetric construction (PPVC) high-rise building”, *Proceedings of the 12th International Conference on Advances in Steel-Concrete Composite Structures*, València, Spain, June.

Court, P.F., Pasquire, C.L., Gibb, G.F. and Bower, D. (2009), “Modular assembly with postponement to improve health, safety, and productivity in construction”, *Practice Periodical on Structural Design and Construction*, **14**(2), 81-89.

Deng, E.F., Yan, J.B., Ding, Y., Zong, L., Li, Z.X. and Dai, X.M. (2017), “Analytical and numerical studies on steel columns with novel connections in modular construction”, *Int. J. Steel Struct.*, **17**(4), 1613-1626.

Gunawardena, T., Ngo, T. and Mendis, P (2016a), “Behaviour of multi-storey prefabricated modular buildings under seismic loads”, *Earthq. Struct., Int. J.*, **11**(6),1061-1076.

Gunawardena, T., Ngo, T., Mendis, P. and Alfano, J. (2016b), “Innovative flexible structural system using prefabricated modules”, *J. Architect. Eng., ASCE*, **22**(4), 05016003.

Ha, T.H., Cho, B.H., Kim, H. and Kim, D.J. (2016), “Development of an efficient steel beam section for modular construction based on six-sigma”, *Adv. Mater. Sci. Eng.*, 1-13.

Han, L.H., Li, W. and Bjorhovde, R. (2014), “Developments and advanced applications of concrete-filled steel tubular (CFST) structures: members”, *J. Constr. Steel Res.*, **100**(1), 211-228.

Hoang, A.L. and Fehling, E. (2017), “Analysis of circular steel tube confined UHPC stub columns”, *Steel Compos. Struct., Int. J.*, **23**(6), 669-682.

Jaillon, L., Poon, C.S. and Chiang, Y.H. (2009), “Quantifying the waste reduction potential of using prefabrication in building construction in Hong Kong”, *Waste Management*, **29**, 309-320.

Kamali, M. and Hewage, K.N. (2016), “Life cycle performance of modular buildings: A critical review”, *Renew. Sustain. Energy Rev.*, **62**, 1171-1183.

Lacey, A., Chen, W., Hao, H. and Bi, K. (2018), “Structural response of modular buildings – An overview”, *J. Build. Eng., ASCE*, **16**, 45-56.

Lam, D. and Williams, C.A. (2004), “Experimental study on

concrete filled square hollow sections", *Steel Compos. Struct., Int. J.*, **4**(2), 95-112
Lawson, M. and Ogden, R. (2008), "'Hybrid' light steel panel and modular systems", *Thin-Wall. Struct.*, **46**, 720-730.
Lawson, M., Ogden, R. and Bergin, R. (2012), "Application of modular construction in high-rise buildings", *J. Architect. Eng.*, **18**(2), 148-154.
Lawson, M., Ogden, R. and Goodier C. (2014), *Design in Modular Construction*, (1st ed.), CRC Press Taylor and Francis Group, Boca Raton, FL, USA.
Liew, R, Lam, D. and Chung, K.F. (2012), "Special issue on advances in steel-concrete composite structures foreword", *Adv. Struct. Eng.*, **15**(9), 1.
Liew, J.Y.R., Dai, Z and Wang, Y. (2016), "Prefabricated prefinished volumetric construction in high-rise buildings", *Proceedings of the 11th Pacific Structural Steel Conference*, Shanghai, China, October.
Liew, J.Y.R., Dai, Z and Chua, Y.S. (2018), "Steel concrete composite systems for modular construction of high-rise buildings", *Proceedings of the 12th International Conference on Advances in Steel-Concrete Composite Structures*, València, Spain, June.
Matoski, A. and Ribeiro, R.S. (2016), "Evaluation of the acoustic performance of a modular construction system: case study", *Appl. Acoust.*, **106**, 105-112.
Monash University (2017), *Handbook for the Design of Modular Structures*, Monash University, Melbourne, Victoria, Australia.
Pang, S.D., Liew, J.Y.R., Dai, Z. and Wang, Y. (2016), "Prefabricated prefinished volumetric construction joining techniques review", *Proceedings of the Modular and Offsite Construction Summit*, Edmonton, Canada, September.
Quale, J., Eckelman, M.J., Williams, K.W., Sloditskie, G. and Zimmerman, J.B. (2012), "Comparing environmental impacts of building modular and conventional homes in the United States", *Res. Anal.*, **16**(2), 243-253.
Ren, Q.X., Hou, C., Lam, D. and Han, L. (2014), "Experiments on the bearing capacity of tapered concrete filled double skin steel tubular (CFDST) stub columns", *Steel Compos. Struct., Int. J.*, **17**(5), 667-686.
Shahtaheri, Y., Rausch, C., West, J., Haas, C. and Nahangi, M. (2017), "Managing risk in modular construction using dimensional and geometric tolerance strategies", *Automat. Constr.*, **83**, 303-315.
Smith, R.E. (2011), *Prefab Architecture: A Guide to Modular Design and Construction*, John Wiley & Sons, Hoboken, NJ, USA.
Taghaddos, H., Hermann, U., AbouRizk, S. and Mohamed, Y. (2014), "Simulation-based multiagent approach for scheduling modular construction", *J. Comput. Civil Eng.*, **28**(2), 263-374.
Vector Praxis (2011), Tall modular building system; Vector Praxis, Toronto, Canada. URL: http://www.vectorpraxis.com/project-details/Tall_Modular_Building_System/101175
Wang, J., Uy, B. and Li, D. (2018), "Analysis of demountable steel and composite frames with semi-rigid bolted joints", *Steel Compos. Struct., Int. J.*, **28**(3), 363-380.

Nomenclature

L_1, L_2	column length of the tenon strengthened part and the un-strengthened part
EI_1, EI_2	bending stiffness of the tenon strengthened part and the un-strengthened part
P	buckling load of the column
P_m	buckling load of a tenon-connected column
P_o	buckling load of a reference pinned-pinned column without tenon
M	bending moment
αL	eigenvalue in characteristic equations, satisfying $P = \alpha_1^2 EI_1 = \alpha_2^2 EI_2$
k	rotational stiffness (unit: Nm/rad)
θ	rotation angle at the bottom end of the column
D	external side width of a square section
d	internal side width of a square section
h	height of a module, equals to $2(L_1+L_2)$
m	relative bending stiffness ratio
n	relative length ratio
λ	relative rotational stiffness ratio
χ	aspect ratio of a module unit, reflecting the geometry uncertainty
ξ	bending stiffness modification factor, reflecting the shear slip uncertainty
φ	rotational stiffness uncertainty factor
E_s, E_c	elastic modulus for steel and concrete material
β	section modulus ratio
δ	error of the numerical results against the theoretical ones
μ	effective length coefficient

DL